Development Trend of Wind Power Technology

John Yan[1], Gang Li[2], Kan Liu[3]

[1]Talos Industry Crop., Marlborough, USA
[2,3]Department of Mechanical Engineering, University of Maryland Baltimore County, USA

***Abstract*— *This paper describes the main types of the state-of-the-art wind energy harvesting technologies and their commercial prospects, and presents shortcomings of Betz's limit and misleading of the blade element-momentum theory for aerodynamic design and computational fluid dynamic simulation of vertical-axis wind turbines. A new aerodynamic design method for vertical-axis wind turbines is presented. A modular, combined, and low-cost wind turbine solution ("super turbine") is developed based on the new aerodynamic design method. By comparing of levelized costs of energy of the super turbine and other wind energy harvesting technologies, the development direction of the new wind energy harvesting technology is explained.*

***Keywords*— Betz's limit, blade element-momentum theory, wind power, attack angle regulation.**

I. INTRODUCTION

The year 2019 is the 100th anniversary of Betz's law. Till this year, wind energy harvesting technologies have been developing for nearly one hundred years. Traditional horizontal-axis wind turbines (HAWTs) have been considered as the mainstream wind energy harvesting technology, which have similar design ideas and configurations. Thus, those HAWTs have resemblances in aerodynamic performances. Since blades of a HAWT rotate in a two-dimensional (2D) plane, each blade has the same aerodynamic performance when the blade rotates to different azimuths. If the HAWT is well designed, the power generation efficiency of the tip region of the blade can reach the maximum value of 59.3% based on Betz's law [1] or computational fluid dynamic (CFD) simulation. Besides the traditional HAWT technology, various vertical-axis wind turbines (VAWTs) have been developed in the last decade. Different types of VAWTs have been designed based on different configurations of blades, including lift-driven based, drag-driven based, and lift- and drag-driven hybrid based blades [2,3]. Due to the misleading of traditional HAWT design and the tip speed ratio (TSR) in the blade element-momentum (BEM) theory [4,5] for VAWT applications, only a few of VAWTs can achieve high wind energy harvesting efficiency and over-speed regulation protection. Some VAWTs cannot harvest enough wind energy under low wind speed conditions and may disintegrate under high wind speed conditions.

Some other wind energy harvesting technologies, such as airborne turbines, wind tunnel turbines, and vortex bladeless turbines, have also been developed. The key challenge of airborne turbine technologies [6] is power transmission, which transmits power (electricity or mechanical power) from a wind turbine at a high altitude to the ground. The levelized cost of energy (LCOE) of airborne turbines will be increased due to their high operations and maintenance (O&M) costs. Therefore, the airborne turbine technologies are difficult to be commercialized now or in the future. Wind tunnel turbines are developed by using a wind tunnel with nozzle design. The basic design concept of a wind tunnel turbine is that the wind tunnel can increased wind speeds and a turbine can increase its harvesting efficiency [7]. However, since the air pressure in the wind tunnel is much higher than that of outside, the airflow is difficult to enter the wind tunnel. Hence, the wind speed at the entrance of the wind tunnel is much lower than the far-field wind speed. The actual generated power and power coefficient of the wind tunnel turbine is much lower than its theoretical design value. Vortex bladeless turbines are developed to harvest wind energy based on vortex effects and rod resonance [8]. Since the energy density of vortex bladeless turbines is very low under non-resonant conditions, the key of the vortex bladeless turbine technology is to make the rod resonate with vortex effects. However, swing frequencies of the rod depend on the wind frequency, and it is difficult for rods to resonate under most natural wind conditions. Hence, the vortex bladeless turbine technology is also difficult to be commercialized.

There is a new research and develop trend to study lift-driven VAWTs since 2015. New lift-driven VAWTs are developed based on an active real-time attack angle regulation technology [9]. Therefore, no matter what technology is developed for wind energy harvesting, the key point is to reduce the LCOE. Only wind energy harvesting technologies with lower LCOE can dominate the wind power market in the future.

II. MAIN FEATURES OF HAWTS

The traditional HAWT technology has been developed to a proven level. However, except for the larger and larger output power, there is no innovative idea in this area. Currently, all manufacturing companies of HAWTs do not provide the trajectory of wind speeds and the output power and design parameters of their HAWT products, such as the diameter of the HAWT, the rated wind speed, and the rated power. The reason is that wind power is the cubic function of the wind speed, and in reality, wind speed is the average wind speed. The energy density of the average wind speed is much higher than the constant wind speed [10]. Under limited conditions, the wind energy of the average wind speed can be quadruple as a constant wind speed. For instance, at normal atmospheric pressure, the wind energy with a constant speed of 5 m/s for 2 hours per square meter is about 153.125 W·h. If the wind speed in one hour is 10 m/s and in another hour is 0, the average wind speed is still 5 m/s, but the energy for these two hours is about 612.5 W·h, which is about quadruple as the constant wind speed. Therefore, the energy is about the frequency of the wind. Based on the experiment, the ratio between the energy of average wind speed and the constant wind speed is about 1.5 to 2.0. That is the most important reason that wind speed and power trajectory cannot represent the aerodynamic performance of wind turbines.

Another reason is that the TSR of the HAWT will exceed the optimal value in the BEM theory that is 5 to 6 with the larger and larger output power of a single HAWT. The TSR of a HAWT product of a Chinese company is close to 10, which is almost doubled the TSR in the BEM theory. Additionally, the customer can calculate aerodynamic performances of HAWTs based on design parameters provided by manufacturing companies, e.g., the power generation efficiency, and compare these aerodynamic performances with actual aerodynamic performances.

The aerodynamic efficiency of a wind turbine is relative to the length of blades. The aerodynamic efficiency of the HAWT can reach the maximum value of 50% at the tip part of a blade when the blade is well designed. However, power generation efficiencies of different positions of the blade get lower with closing to the root part of a blade. The power generation efficiency of the root part of the blade is almost zero. Considering low efficiency of mechanism and electricity and wind power loss, the power generation efficiency of HAWTs is hardly higher than 25% [11]. The LCOE of the HAWT mainly depends on two aspects, i.e., the cost of facilities of a wind turbine and the power generation efficiency. Once those two aspects are determined, the LCOE of the HAWT only varies with wind conditions of a wind farm. Wind turbines are mechanical products, and their costs cannot drop quickly as electronic products.

III. TRADITIONAL VAWTS

Blades of traditional lift-driven VAWTs are fixed. Attack angles of blades can be only changed by centrifugal forces of blades when the wind speed is higher than cut-off speeds of traditional lift-driven VAWTs, as shown in Fig. 1. Attack angle changes of blades of traditional VAWTs cannot improve their aerodynamic efficiency, but protect VAWTs by reducing their aerodynamic efficiency when the wind speed is higher than cut-off speeds of VAWTs. Since attack angle control of blades of traditional VAWTs is achieved by using elastic components, diameters of traditional VAWTs are small, as shown in Fig. 2. Generally, traditional VAWTs can be only designed for small-scaled wind turbines, whose rated power is lower than 10 kW.

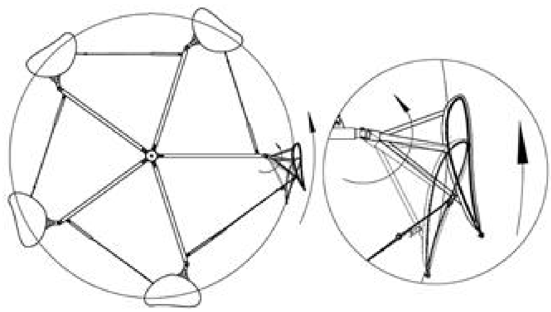

Fig. 1: Structural diagram of a VAWT using centrifugal forces for over-speeding protection

There are five steps in design procedures of these lift-driven VAWTs. (1) Blade selection. The blade airfoil must select an asymmetrical low-speed airfoil instead of the symmetric airfoil, such as NACA0012, NACA0015, and NACA0018 [12]. (2) Concave direction. The concave side of the centerline of a blade is outward instead of the convex side. (3) Attack angle design. The attack angle of the blade should be design within 4 to 8 deg. (4) Design of the ratio of the blade width to the diameter of the lift-driven VAWT. The optimal ratio of the blade width to the

https://dx.doi.org/10.22161/ijaers.76.15 ISSN: 2349-6495(P) | 2456-1908(O)

diameter of the lift-driven VAWT should be 0.16 to 0.165. This ratio is not the solidity of HAWTs. The optimal TSR of blades of a VAWT with a fixed attack angle is between 1.4~1.5 [13] not 4.0~6.0, which is designed based on Darrieus VAWT theory. It is this misleading conclusion that makes shapes of lift-type VAWTs varied. (5) Number of the blades. Based on experimental results, VAWTs with five blades perform the best harvesting efficiency of wind energy.

Fig. 2: A VAWT with relatively fixed blade angles

Many researchers work on CFD simulation of VAWTs with a fixed attack angle. However, since turbulence of VAWTs is complicated, there are differences between CFD simulation results and actual aerodynamic performances of VAWTs [14]. CFD simulation of VAWTs should be improved based on further understanding of the aerodynamic characteristics of blades at different positions and the turbulent characteristics of VAWTs.

In order to simulate aerodynamic performances of VAWTs by current CFD software, a static CFD method is developed. Detailed processes of the static CFD method are described below. 1) Determining design parameters of the VAWT, including the airfoil, the blade chord, the blade length, the diameter of the VAWT, blade installation orientation, and installation angles of blades. 2) Predesigning the rotation speed of the VAWT for different wind speeds to calculate the combination speed of the rotation speed of the VAWT and the wind speed at different positions (or azimuth angles). 3) Simulating the lift-driven torque of the blade at the position (or azimuth angle) with the combination speed. In order to accurately calculate a total lift-driven torque of the blade for one revolution, one can simulate the lift-driven torque of the blade for each degree (or every 5 or 10 deg) and calculate the average value of lift-driven torques of the blade at different positions.

IV. ACTIVE REAL-TIME ATTACK ANGLE REGULATION TECHNOLOGY

For a VAWT with fixed blades, the attack angle of each blade continuously changes with the change of blade position due to the rotation of the VAWT. The magnitude and the direction of its torque of each blade also change with the change of its attack angle. At some positions, the toque of the blade is negative. Since the final output torque of the VAWT is the sum of torques of all blades, the aerodynamic efficiency of the VAWT is not very high

The wind energy harvesting efficiency of a VAWT can be improved by controlling attack angles of its blades based on the position of blade, the rotation speed of VAWTs, the wind direction, the wind speed, and power of the VAWT, as shown in Fig. 3. Additionally, the output power of the VAWT can be adjusted to be constant when the rotation speed of the VAWT is variable or over-speeding.

An active real-time attack angle regulation technology of VAWTs is developed to maximize wind energy harvesting efficiency by adjusting the attack angle of each blade. The control motion of attack angles of blades can be achieved by using rotating shaft supporting mechanism and servo motors. The active real-time attack angle regulation technology is different from the pitch control technology of HAWTs since the attack angle a blade of the VAWT is a vector quantity, but the blade pitch of a HAWT is a scalar quantity.

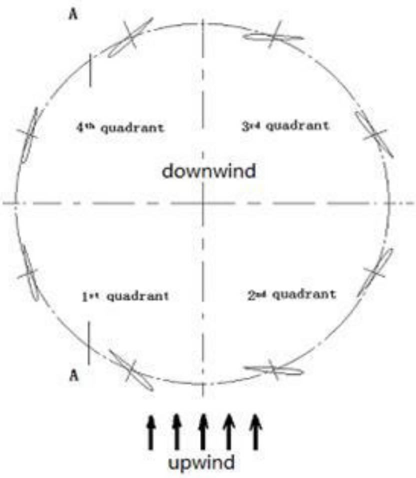

Fig. 3: Attack angles of a blade of the VAWT at different quadrants

A wind energy harvesting test of a VAWT with the active real-time attack angle regulation technology was conducted in a wind tunnel, as shown in Fig. 4. The blade length the diameter of the VAWT is 1 m and 1.36 m,

https://dx.doi.org/10.22161/ijaers.76.15 ISSN: 2349-6495(P) | 2456-1908(O)

respectively. The load of the VAWT is generated by a magnetic brake. The cross-sectional area of the wind tunnel is 10 m^2. When the wind speed was 2 m/s, the rotation speed of the VAWT was 44 rpm and the output torque of the VAWT was a constant value of 1 Nm. Test results showed the power generation efficiency of the VAWT with the active real-time attack angle regulation technology was about 68% (ignore the blockage ratio), which was higher than Betz limit. Betz limit is used for designing blades of HAWTs that rotate in a 2D single-disk plane. Since blades of the VAWT with controllable attack angles can harvest wind energy from the upwind and the downwind, the VAWT with the active real-time attack angle regulation technology actually harvests wind energy in a three-dimensional multi-disks space [12]. When the VAWT in the upwind and downwind directions are unfolded separately, it is equivalent to a HAWT in a plurality of 2D plane, as shown in Fig. 5.

The power generation efficiency of VAWTs with the active real-time attack angle regulation technology can be significantly improved by adjusting attack angle of blades. Even if the VAWT adopts the active real-time attack angle regulation technology, the power generation efficiency of VAWTs can greatly changes with changes of the attack angle setting at different positions.

Fig. 4: Wind tunnel test of a VAWT with active real-time attack angle regulation technology

The TSR of the VAWT in this wind energy harvesting test was 1.6, which is much lower than the TSR designed by the BEM theory, where the optimal value of the TSR is 5~6 and the minimum value of the TSR is 3, as shown in Fig. 6. The TSR of the VAWT in this wind energy harvesting test was also much lower than the TSR of a HAWT. Therefore, the optimal TSR in the BEM theory is incorrect and cannot be used for VAWT design. This is the reason why there are so many configurations of VAWTs nowadays.

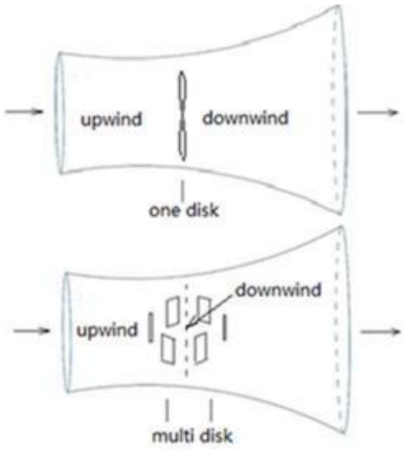

Fig. 5: Schematic diagram wind energy harvesting tests for single-disk and multi-disk

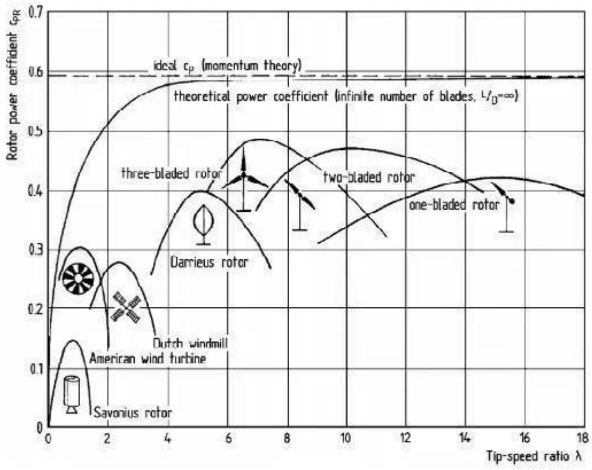

Fig. 6: TSRs of different wind turbines based on BEM theory

V. VAWTS WITH ACTIVE REAL-TIME ATTACK ANGLE REGULATION

Active real-time attack angle regulation of VAWTs can make each blade has the optimal angle of attack at any position, and maximize wind energy harvesting efficiency of VAWTs. When the wind in the upwind direction passes through the first half of the VAWT and reaches the inside of the VAWT, it becomes the downwind direction similar to the HAWT and the wind speed decreases. Hence, the power generated by the blades in the second half of the VAWT is much lower than the work done by the blades in the first half of the VAWT. Magnitudes of the power generated by blades at different positions are also different. The moment generated by the blade in the first quadrant is much larger than the moment generated by the blade in the fourth quadrant. Similarly, the moment generated by the

https://dx.doi.org/10.22161/ijaers.76.15 ISSN: 2349-6495(P) | 2456-1908(O)

blade in the second quadrant is also much larger than the moment generated by the blade in the third quadrant.

Wind energy can be represented by a function of the cube of the wind speed. If the wind speed in the downwind direction inside the VAWT can be recovered to the upwind speed, the wind energy utilization rate of the VAWT can be higher than 68%. Due to aerodynamic characteristics of the wind, the wind speed will gradually recover to the original wind speed under the action of subsequent wind when the wind passes through an object. If the diameter of the wind turbine is infinite and the blade height is sufficiently low, the wind will gradually recover to the original wind speed after passing through blades in the upwind direction. Hence, blades in the downwind direction can be affected by the same wind as the blades in the upwind direction, as shown in Fig. 5.

In order to achieve the wind speed recovery in the downwind direction of the VAWT, the VAWT should be designed based on the ratio of the diameter of the wind turbine and the blade length that is set to more than 10. In most of the third and fourth quadrants, the wind speed will be recovered. The wind energy harvesting efficiency of VAWTs can be greatly improved, which is higher than 68%.

The costly components in the VAWT system are the generator, the wind turbine support structure, and turbine blades. If lower costs of these three components and higher wind energy harvesting efficiency can be achieved, the LCOE of wind turbines can be greatly reduced. This is the basic design concept of a super turbine [15].

VI. SUPER TURBINE DESIGN

A super turbine is composed of a series of π-shaped steel structures with the same specification to form an annular support system. Dozens or hundreds of sets of blades, which are similar to sails, are fixed on movable trolleys. The trolleys move on a circular track. The attack angle of each blade can be adjusted by active real-time control. Each blade connects to its two neighboring blades through two steel cables and a chain. A plurality of small high-speed generators, which are fixed on the circular track, are driven by a chain-pinion system to generate electricity. Multiple currents are collected through a combiner box and supplied to a medium-sized power inverter for grid-connected power generation. Super turbines are completely different from existing wind turbine technologies. Regardless of turbine blades, transmission systems, generators, the support structure, and grid-connected systems are different from traditional wind turbines.

VII. STRUCTURE OF THE SUPER TURBINE

According to wind conditions of the wind farm, the site environment, and customer needs, the power generation capacity of the super turbine can be scaled from 7 MW to 50 MW. If the track of the super turbine is designed to be oval, the long axis direction is taken as the windward direction. The steel structure used for each span of the track is in the same size. The size of the super turbine can only change with changes of the number of spans of the track.

The super turbine includes six major subsystems, which are the steel structure support and track system, the turbine blade positioning system, trolleys, the hydraulic and transmission system, the active real-time control system, the grid connection system, and the monitoring system.

7.1 Steel structure support structure and towers

The tower and the steel structure are composed of standard 70 H-shaped steel. The height of each tower is 20 m. The distance between two neighbouring towers is 20 m. The beams form a π-shaped network support structure, as shown in Fig. 7.

7.2 Circular track

The existing standard No. 15 light rail is used to build the track of the super turbine. Three sets of tracks are set on H-type beams at different positions. Each trolley has six customized wheels, but only four wheels can contact the track at the same time. It can ensure the stable operation of the trolley and reduce the frictional resistance of the trolley.

Fig. 7: Towers and supporting structures of the super turbine

7.3 Turbine blades

Turbine blades are manufactured by FRP pultrusion process. The height of each turbine blade is 11.5 m, and the width of each turbine blade is 2.6 m. It is divided into upper and lower blades, and the weight of each turbine blade is 350 kg. The upper blade and the lower blade are coaxially designed. The central axis of the blade passes

https://dx.doi.org/10.22161/ijaers.76.15 ISSN: 2349-6495(P) | 2456-1908(O)

through the center position of the trolley and is rigidly connected to the shaft of the hydraulic rotary motor, so that the angle of the upper blade and the lower blade can be synchronized to change, and sufficient rotation torque can be obtained.

7.4 Turbine blade positioning system

In arc segments of the track, a mechanical and optoelectronic positioning device is arranged every 10 rad, and each trolley is coded (001, 002, 003 ...). When differently coded trolleys pass different positioning devices, locations of different blades are obtained by the positioning device, as shown in Fig. 8.

Under 5G communication conditions, inch-level GPS can also be used to independently position each blade. The advantage of using GPS to locate the blade is that the control system is simpler, but it depends on GPS signals and 5G network. Once the signal is interrupted for a short time, there will be a serious of impacts on the super turbine.

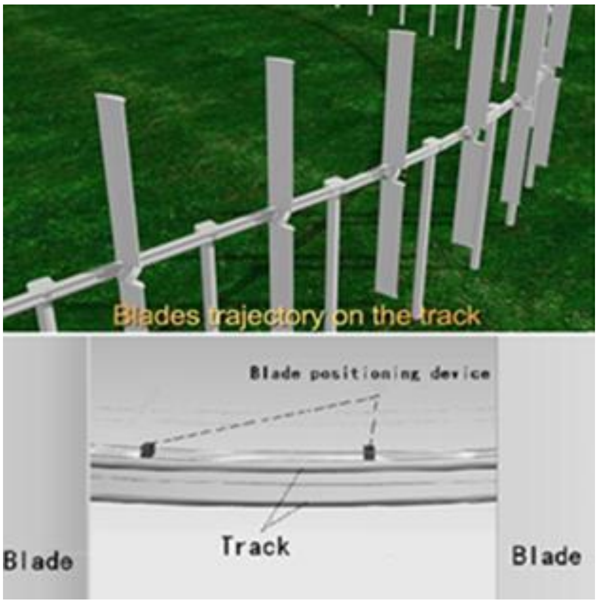

Fig. 8: Turbine blade positioning system of the super turbine

7.5 Trolleys

The body of the trolley is made of cast steel. The cantilever of the trolley is made of forged parts. The rotary shaft of the hydraulic motor in the trolley and shafts of upper and lower blades are rigidly fixed, as shown in Fig. 9. Since the diameter of the super turbine is 255 m, the maximum speed of the trolley on the track cannot exceed 21 m/s, which is equivalent to the rotation speed of 1.6 rpm of the trolley on the track. Since the rotation speed of the blade is very low, rated rotation speed and torque of current motors can satisfy the requirements. When the typhoon is coming, attack angles of blades can be adjusted to minimize the load on the super turbine. At the same time, the trolleys on the track are stopped by brakes.

Fig. 9: Trolley and the track structure of the super turbine

7.6 Generators

Generators that are conventional standard permanent magnet generators with a rated speed of 1500 rpm and the rated power of 100 kW (or 50 kW) are used to maintain low cost and easy replacement. Generators are fixed on the track and vertically installed (or parallel) to the track, which are driven by a chain pinion system at the end of generators and trolleys, as shown in Fig. 10.

7.7 Steel cables and chains

There are two steel cables at upper and lower ends of trolleys, which connect two adjacent trolleys. The steel cables is used to tow the trolleys, and two adjacent trolleys are connected to each other by a chain. The back of each trolley is made into a gear type, so that the chain can be made into segments, and the length of each chain is the trolley spacing. If the track with the diameter of 255 m allows the chain to be bent, generators can be horizontally placed (parallel to the horizontal line) to facilitate maintenance.

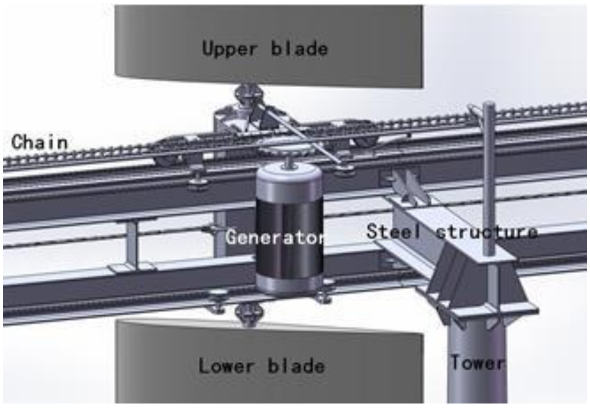

Fig. 10: Generators, the chain, and the supporting structure of the super turbine

https://dx.doi.org/10.22161/ijaers.76.15 ISSN: 2349-6495(P) | 2456-1908(O)

7.8 Central Control Unit

The central control unit is composed of multiple sets of motion controllers or PLCs. One motion controller controls the movement of a trolley. The advantage is that any group of motion controllers or trolleys does not affect the function of other trolleys, which can ensure the whole super turbine system continuously working. The disadvantage of this control solution is the cost of the central control unit is relatively high. Another control solution is to use a motion controller to control the trolley with the number 001, and the trolley with the number 002,003, ... follows the movement of the trolleys with the number 001. The advantage of the control solution is that the cost is low, and the shortage is that if the motion controller fails or the trolley numbered 001 fails, the entire system will stop running.

The second design scheme but use two motion controllers, and the second motion controller is used as a backup controller. Which scheme is adopted will be determined through comprehensive evaluation after specific design and trial operation on a computer.

7.9 Collection and grid connection

As 50-kW or 100-kW grid-connected power inverters are already popular products, their costs are lower. The AC permanent magnet generators are connected to one or two grid-connected power inverters and then connected to the grid after AC-DC conversion, as shown in Fig. 11.

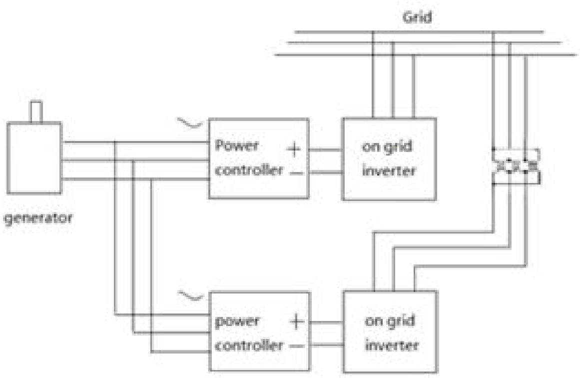

Fig. 11: On grid logic diagram of the super turbine

VIII. FEATURES OF THE SUPER TURBINE

The design of the super turbine can be customized based on wind conditions, site conditions, and customer needs. The diameter of a circular track and the swept area of a blade of the minimum super turbine are 255 m and 18,400 m^2, respectively. The rated power of the minimum super turbine is 7 MW. The maximum super turbine can be scaled up to 50 MW with an oval-shaped track, as shown in Fig. 12. If the wind direction of a wind farm is relatively constant, such as the southeast wind in summer and the northwest wind in other seasons, one can choose the oval-shaped super turbine for wind energy harvesting. If the wind direction of the wind farm frequently varies with weather changes, one can choose the circular-shaped super turbine for wind energy harvesting.

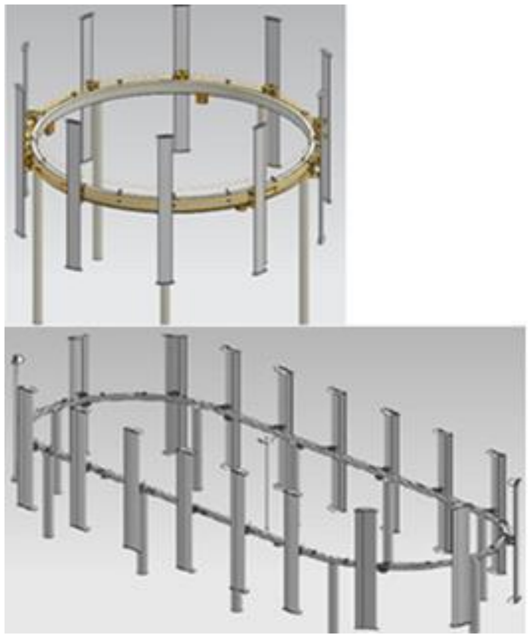

Fig. 12: Shapes of super turbines for different wind conditions

Table. 1: Costs of components of a 7 MW super turbine

Components	Type / Size	Price	Quantity	Total cost
Turbine blades	350 kg	$4,500	120	$540,000
Trolleys	-	$8,000	60	$480,000
Generators	100 kW	$5,000	70	$350,000
Support structure	4000 kgs	$4,500	40	$180,000
Track	8500 kgs	$10,000	40	$400,000
Power inverter	100 kW	$70,000	8	$560,000
Control unit	-	-	1	$200,000
Cables	-	-	-	$100,000
Others	-	-	-	$200,000
Total price	-	-	-	$3,010,000

Table. 2: Power generation costs of a 7 MW super turbine under different wind conditions

Average wind speed (m/s)	Annual power generation (MWh)	Total generation in 20 years (MWh)	20 years income ($)	Cost of per MWh ($)	Cost of per KWh ($ cent)
5	7,500	150,000	18,000,000	24.0	2.40
5.5	9,800	196,000	23,520,000	18.4	1.84
6	12,800	256,000	30,720,000	14.1	1.41
6.5	16,200	324,000	38,880,000	11.1	1.11
7	20,300	406,000	48,720,000	8.9	0.89
7.5	25,000	500,000	60,000,000	7.2	0.72
8	30,300	606,000	72,720,000	5.9	0.59
8.5	36,400	728,000	87,360,000	4.9	0.49
9	43,200	864,000	103,680,000	4.2	0.42
9.5	50,800	1,016,000	121,920,000	3.5	0.35
10	59,200	1,184,000	142,080,000	3.0	0.30

A 7 MW super turbine is developed by using standardized components, including a circular track with the diameter of 255 m and an effective swept area of 18,400 m^2, 60 sets of turbine blades, and 70 100 kW permanent magnet generators. The total cost of the 7 MW super turbine is $3.5 million, including costs of construction and installation. The comprehensive cost per watt is only $0.5. In addition to lower capital costs and operation and maintenance costs, the overall cost of the super turbine will be only one third of a traditional 7 MW HAWT.

Table 2 shows the LCOE of a 7 MW super turbine under different wind conditions. The construction cost of the super turbine is $3.6 million. The LCOE of the super turbine is ¢0.6 - 2.4 / kWh in a wind farm with a wind speed of 5~8 m/s. Due to low costs of investment, operation, and maintenance of super turbines under the same scale, the LCOE will be much lower than that of wind farms using traditional wind turbines. Super turbines can make profits without any subsidies, making wind power investment shift from policy-driven to capital-driven.

IX. CONCLUSION

Electricity power is a special commodity. In addition to the quality of electricity, the LCOE of wind turbines is the most important economic indicator of power plants. In the future, wind power technology, which does not rely on various subsidies and has lower LCOE than those of thermal power and hydropower technologies, is the future development direction of the wind power technology

ACKNOWLEDGEMENTS

The author would thank Mr. Gregory Swecker, who is the owner of SWECKER FARM at Iowa state in the United States, for his supports of the super turbine.

REFERENCES

[1] Betz A. (1966). Introduction to the Theory of Flow Machines. London: Oxford: Pergamon Press.

[2] Ma XS. Gao R. and Chen H. (2007). Summarize of the history of generatating power by wind and comparison of some kings of wind turbine. *Technology of Practical Energy*, 9, 24-27.

[3] Mo XD. and Li T. (2010). Types and development advantage of vertical axis wind turbine. *Energy Conservation Technology*, 28(5), 450-453.

[4] Zhou ZZ. Feng J. Li Y. and Yu YY. (2011). *Principles and Applications of Wind Turbines*, Beijing: China Water & Power Press.

[5] Salameh Z. (2014). *Renewable Energy System Design*, Duxford: Elseiver.

[6] Acher C. L. and Calderia K. (2009). Global assessment of high-altitude wind power. *Energies*, 2(2), pp. 307-319.

[7] Chen WQ. Lv D. Jing J. Chen WL. and Lu XD. (2006). The new wind power generation setting of collect energy. *Shanghai Energy Conservation*, 6, 16-18.

[8] García C. Carlos J. Guillaume H. Yáñez D. J. and Mier-Torrecilla M. (2016). SHAPE project vortex bladeless:

https://dx.doi.org/10.22161/ijaers.76.15 ISSN: 2349-6495(P) | 2456-1908(O)

Parallel multi-code coupling for fluid-structure interaction in wind energy generation, *Partnership for Advanced Computing in Europe*, Barcelona.

[9] Yan Q. (2014). Feasibility study on large vertical axis wind turbines, *Industry of Wind Energy*, 2, 12-14.

[10] Yang G. Du YX. and Chen M. (2008). The calculation of energy provided by wind turbine based on its power characteristic and the wind frequency weibull distribution, *Journal of Electric Power*, 4(23), 276-278.

[11] Yan Q. and Jiang CQ. (2006). On the horizontal axis wind turbine's efficiency, Shanghai Aeolus Windpower Technology Co., Ltd. (SAWT), Shanghai.

[12] Paraschivoiu I. (2002). *Wind Turbine Design with Emphasis on Darrieus Concept*, Montréal: Polytechnic International Press, 2002.

[13] Yan J. (2012). Current and future vertical wind turbine. *Wind Power*, 5, 50-53.

[14] Khalid SS. Zhang L. Zhang XW. and Sun K. (2013). Three-dimensional numerical simulation of a vertical axis tidal turbine using the two-way fluid structure interaction approach. *Journal of Zhejiang University SCIENCE A*, 14, 574-582.

[15] Yan Q. Circuit wind power system and method for generating electricity using the same. US Patent 9396226.